ELSEVIER

Polymer 42 (2001) 2597–2609

polymer

www.elsevier.nl/locate/polymer

Crystallization of poly(ethylene oxide) in a photopolymerizable monomer under an electric field

C. Park[1], R.E. Robertson*

Department of Materials Science and Engineering, Macromolecular Science and Engineering Center, The University of Michigan, Ann Arbor, MI 48109-2136, USA

Received 19 April 2000; received in revised form 24 July 2000; accepted 27 July 2000

Abstract

The miscibility behavior and crystallization of poly(ethylene oxide) (PEO) from two non-polar solvents when subjected to a high electric field were studied. The two solvents, both photopolymerizable, were urethane dimethacrylate (UDMA) and 1,6-hexanediol dimethacrylate (HDDMA). The electric field was found to decrease miscibility in at least HDDMA, causing liquid–liquid phase separation at temperatures above the PEO melting temperature and well above the dissolution temperature. Cooling the solutions below 45°C under the field caused the irregular spherulites forming in HDDMA (a low-viscosity solvent) to align in groups and, above 0.2 kV/mm, to elongate. Lamellae within the spherulites tended to align with their planes in the field direction. Only branched lamellae formed in UDMA (a high-viscosity solvent), with the longest lamellae in the field direction and the few branches at large angles to these. For both solvents, crystallization was retarded slightly by the field, as was the total amount of crystallinity in HDDMA, and possibly also in UDMA. PEO crystallinity in UDMA was much less than that in HDDMA, with or without the field, presumably because of viscosity.

Keywords: Poly(ethylene oxide); Electric fields; Crystal alignment

1. Introduction

Modification of materials using external forces, such as shear, electric, magnetic, thermal, and photonic, have received much attention for tailoring structures for specific demands. Among them, electric fields have often been employed to create anisotropic structures and to attain desirable actuation in response to a stimulus with ferroelectrics, nonlinear optics, liquid crystals, and electrorheological fluids. The morphology of polymer melts and blends under an electric field has been reported [1–9]. Polymers having permanent dipoles or high dielectric constants, such as poly(vinylidene fluoride), poly(ethylene oxide) (PEO), and polyamides, have often been used for these studies [1,3–6,8]. Diblock copolymer solutions having relatively large dielectric constant mismatch between the blocks and solvents were also used to study the effects of electric fields on the polymer morphology [10–13]. Aligned PEO phases from diblock copolymers [10–12] and a fibrillar, thread-like PEO structure in a blend of poly(styrene-*b*-ethylene oxide) and poly(styrene) with a ternary solvent mixture [13] were observed under an electric field during solvent casting. Alignment of cylindrical microdomains of a poly(styrene-*b*-methyl methacrylate) diblock copolymer under an electric field was also demonstrated using transmission electron microscopy and small angle neutron scattering [14,15]. Liquid crystalline polymer, having rod-like, plank-like, or disk-like mesogen structures, can be aligned as well under an electric field, producing anisotropic polarization [16]. Electric field-induced alignment of rod-like structures (fibers) and platelets in particulate composites was studied by the authors [17]. Platelets were found to align more efficiently than rod-like structures. Since crystalline lamellae have a platelet shape, they may also align readily in an applied electric field of sufficient field strength and application time. A study of the lamellar surface orientation of poly(styrene-*b*-methyl methacrylate) parallel to an electric field was reported by Amundson et al [18–20]. Most studies and observations have been performed in two-dimensional (2D) systems, such as thin layers on a slide glass. These may not accurately represent an actual 3D system.

In the present study, the crystallization of PEO under an electric field was investigated in a 3D system using a photopolymerizable monomer. An AC electric field was

* Corresponding author. Tel.: +1-734-763-9867; fax: +1-734-763-4788.
E-mail address: rer@umich.edu (R.E. Robertson).
[1] Present address: Advanced Materials and Processing Branch, Mail Stop 226, NASA, Langley Research Center, 6 West Taylor St., Hampton, VA 23681, USA.

0032-3861/01/$ - see front matter
PII: S0032-3861(00)00591-7

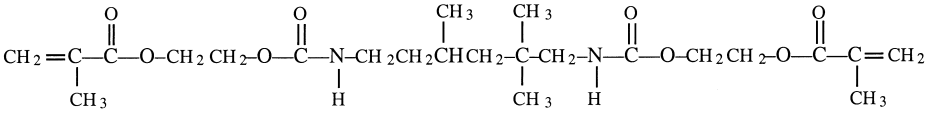

Urethane dimethacrylate

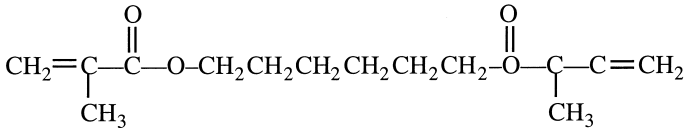

1,6-Hexandiol dimethacrylate

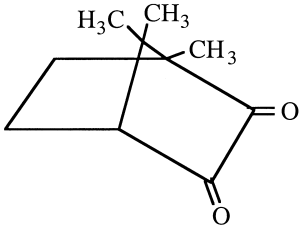

Camphorquinone

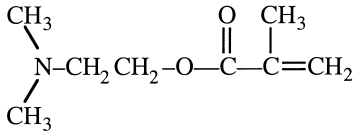

N,N-dimethylaminoethyl methacrylate

Fig. 1. Chemical structures of matrix materials.

applied to PEO solutions in the monomer at an elevated temperature, and crystallization was effected by cooling the solutions while the electric field was being applied. The resulting soft gel was hardened by polymerizing the monomers with blue light. The morphology of the aligned, solid PEO composites was observed in thin sections and at fracture surfaces using light and scanning electron microscopy.

2. Experimental

2.1. Materials

The polymer studied was PEO having a number-average molar mass of ca. 20,000 (g/mol), which was obtained as Polyox from Union Carbide Corp. This was dissolved at elevated temperatures in either of two photopolymerizable monomers, urethane dimethacrylate (UDMA) or 1,6-hexanediol dimethacrylate (HDDMA), which were obtained from Esschem Co. The chemical structures of the monomers are shown in Fig. 1. The viscosities were 12.5 Pa s for UDMA and 7.0×10^{-3} Pa s for HDDMA. The compositions studied were 10 wt% PEO, 90 wt% polymerizable monomer. Both UDMA and HDDMA monomers were able to be polymerized by blue light with camphorquinone as the photoinitiator and *N,N*-dimethylaminoethyl methacrylate as the accelerator. (The structures of these are also shown in Fig. 1.) The monomers were able to be solidified to a depth of 3 mm within about 3 s under illumination by intense blue light.

2.2. Procedures

PEO was dissolved in the monomers at ca. 70°C to form clear solutions. For behavior under an electric field, the solutions were placed in transparent polystyrene cuvet cells having a rectangular cross-section of 10×3.5 mm^2 and 18 mm depth. (The total height of the cell was 45 mm.)

Aluminum plates were used as electrodes in the cuvet cell, and the spacing between them was ca. 7.5 mm. Electric fields of up to 0.80 kV/mm (60 Hz AC) were applied to the solutions. After pouring the solution at 70°C into the cuvet cells, the solution typically began cooling toward room temperature, and the electric field was applied when the temperature had fallen to around 45°C, before PEO crystallization began, unless otherwise noted. The field continued to be applied until a gel had formed and the monomer polymerized. Polymerization was done with a blue light gun (Caulk Dentsply). For isothermal experiments, a silicone oil bath was employed to control the temperature.

To study real-time behavior of the mixture under the electric field before polymerization, a 2D system was employed. PEO/HDDMA (10/90) was placed on a glass slide between brass electrodes spaced 580 μm apart. The electric fields applied to the solution were 1 and 2 kV/mm AC. A heat gun was used as the source of heat. The changes occurring were observed with an optical microscope using

transmitted light and recorded with a CCD camera and a VCR.

2.3. Characterization

Various types of specimens were prepared to access the morphology of crystalline PEO. Thin sections (ca. 150 μm thick) for optical microscopy were prepared by sectioning the polymerized solids parallel to the applied electric field axis using a Buehler Isomet low-speed saw. Fracture surfaces were obtained by cleaving the solids in liquid nitrogen after notching with a razor blade. Fractures were initiated with the fracture plane either parallel or perpendicular to the electric field axis. The fracture surfaces were examined with a Hitachi S-800 scanning electron microscope (SEM).

The melting temperature and heat of fusion of PEO were measured using differential scanning calorimetry (DSC) (Perkin–Elmer DSC 7) at the heating rate of 10°C/min on specimens cooled in room air from 70°C. The dissolution temperatures of PEO crystals in the liquid monomers were monitored using a hot stage and controller (Mettler FP 82 and 80) with an optical microscope (Olympus BH-2).

The segregation of PEO in the solids was assessed by measuring its dissolution in distilled water. A Perkin–Elmer AD-4 Autobalance was employed to measure the weight loss after the polymerized mixture had soaked in distilled water for 72 h. Specimens for this were cut from billets hardened in the cuvet cells and measured 7.5×3.5 mm^2 by 0.7–1.4 mm. The 7.5×3.5 mm^2 surfaces were parallel to the electric field axis, and the 0.7–1.4 mm dimension was along the cuvet cell axis. The weight loss of each was monitored with time and was found to stabilize within 72 h.

Wide-angle X-ray diffraction measurements were made with a Rigaku rotating-anode wide-angle X-ray diffractometer. The X-ray source was Ni-filtered CuKα radiation, and the 2θ-scan was performed between 5 and 70° at the rate of 5°/min at room temperature. Specimens for this were also cut from billets hardened in the cuvet cells and measured 7.5×3.5 mm^2 by 1–2 mm. The 7.5×3.5 mm^2 surfaces were parallel to the electric field axis, and the 1–2 mm dimension was along the cuvet cell axis. The specimen was oriented so that the diffraction plane contained the axis along which the electric field had been applied.

3. Results

3.1. PEO crystallization and morphology

3.1.1. Morphology in liquid monomers without an electric field

PEO crystallization from and dissolution into the photopolymerizable monomers were examined with a hot stage and an optical microscope. PEO crystals usually began to dissolve around 40°C, and with 10% PEO, dissolution appeared to be complete by 45°C at the heating rate of 2°C/min. When clear PEO solutions prepared at 70°C were cooled to room temperature at the rate of 2°C/min, PEO crystals began to appear at around 40°C. Below 40°C, PEO crystallized much more rapidly from HDDMA than from UDMA, probably owing to the three orders of magnitude lower viscosity of HDDMA. Optical micrographs of the crystalline morphology of PEO occurring in thin layers of the unpolymerized monomers without an electric field are shown in Fig. 2. From HDDMA, PEO formed irregular (immature) spherulites (Fig. 2(a)), and from UDMA, PEO formed a branched multi-lamellar structure (Fig. 2(b)). (The ±45° texture in Fig. 2, especially Fig. 2(b), was caused by the orientations of the polarizers.) The crystalline morphology was not affected noticeably by the presence of the initiator and accelerator in either PEO/UDMA (10/90, wt/wt) or PEO/HDDMA (10/90) gels, though gelation in PEO/UDMA seemed to be slightly accelerated. Crystallization in the cuvet cells resulted in the mixture being gelled.

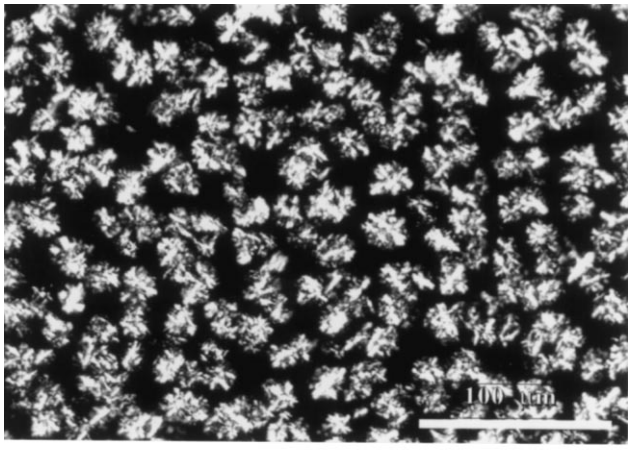

(a)

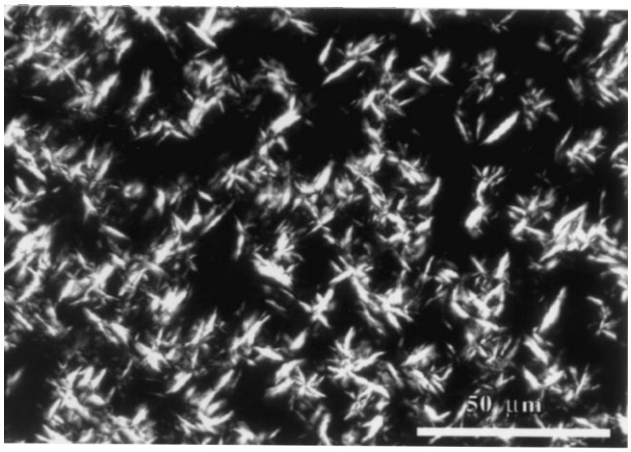

(b)

Fig. 2. Optical micrographs with transmitted light through crossed polarizers of PEO crystallized from thin layers of solution without an electric field: (a) PEO/HDDMA (10/90, by weight); (b) PEO/UDMA (10/90, by weight).

3.1.2. Crystallization and morphology under an electric field

To study PEO crystallization under an electric field, field strengths of up to 0.8 kV/mm, 60 Hz AC, were applied to clear solutions of PEO in either HDDMA or UDMA. The electric field was usually applied after the temperature had fallen from 70 to ca. 45°C. When allowed to cool in room air from 70°C, the PEO/HDDMA (10/90) solution became translucent after ca. 1 min (at ca. 40°C) and completely opaque after ca. 3 min (at ca. 35°C).) When opaque, the mixture was a gel. Gel formation was relatively independent of an electric field, though its rate of formation was slightly retarded by the field.

The solution of PEO in UDMA became translucent after 7–10 min (<30°C) when the solution was allowed to cool from 70°C in room temperature air. The mixture was completely opaque after ca. 30 min, with or without an applied electric field, though gelation tended to be retarded under the electric field. PEO/UDMA (10/90) usually formed more cohesive gels and harder solids after curing than did PEO/HDDMA (10/90). The higher cohesiveness of the PEO/UDMA gel probably arose from the higher viscosity of UDMA. The harder solid after curing probably resulted from the higher hardness of UDMA than HDDMA; e.g. the elastic modulus of pure hardened UDMA was found to be 2.5 GPa, that of a 75/25 mixture of UDMA and HDDMA was 2.0 GPa [21]. The slower gelation of PEO in UDMA than in HDDMA was probably caused also by UDMA's higher viscosity.

Optical micrographs using transmitted light of thin sections of hardened (polymerized) PEO/HDDMA are shown in Fig. 3. When crystallized without an electric field, the immature PEO spherulites (appearing here as black spheres) were randomly distributed (Fig. 3(a)). When crystallized under an electric field of strength greater than ca. 0.2 kV/mm, the spherulites became elongated and organized into groups aligned with the electric field (Fig. 3(b); the electric field (EF) was horizontal, as indicated). The HDDMA phase was polymerized while the electric field continued to be applied. When the electric field strength was below ca. 0.2 kV/mm, the spherulites organized into aligned groups without elongating. Most of the aligned groups of spherulite were parallel to the electric field within an angle of a few degrees.

Example scanning electron micrographs of the fracture surfaces of hardened PEO/HDDMA are shown in Fig. 4. When crystallized without an electric field (Fig. 4(a) and (b)), the PEO formed randomly distributed irregular (immature) spherulites, as was seen in Fig. 3(a). The spherulites were approximately 40 μm in diameter. On the other hand, when crystallized (and the matrix hardened) with an electric field (Fig. 4(c) and (d)), the PEO formed elongated spherulites that were often aligned with other spherulites parallel to the electric field, as was seen in Fig. 3(b). Some of the elongated spherulites were longer than 400 μm. As seen in Fig. 4(e) and (f), even for those crystal lamellae nominally

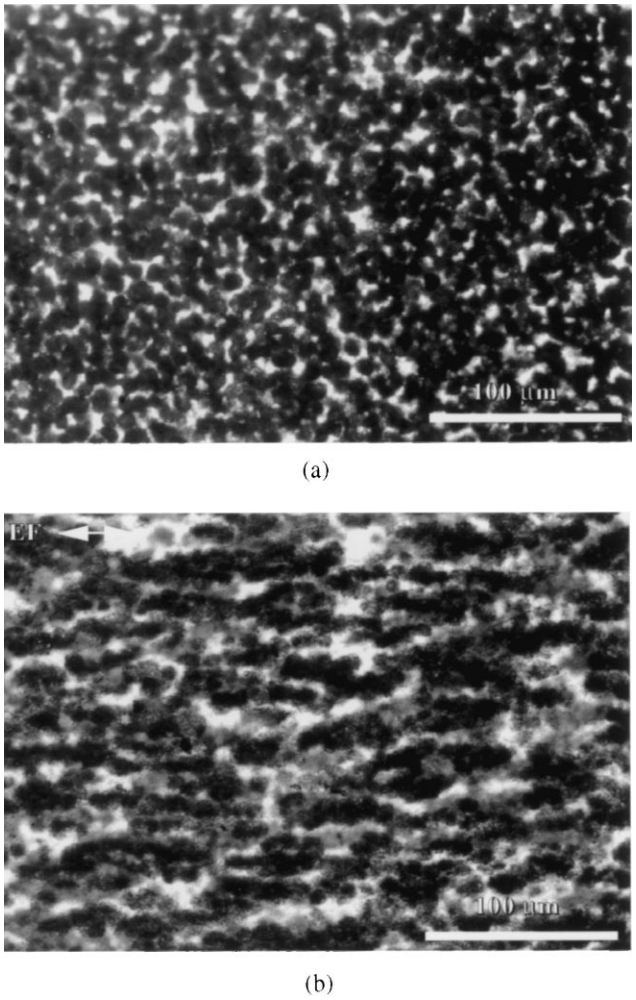

Fig. 3. Optical micrographs of thin sections of PEO/HDDMA (10/90) mixtures gelled (a) without and (b) with an electric field; polymerized after 3 min under 0.8 kV/mm, 60 Hz.

radiating from the spherulite center perpendicular to the electric field axis, their planes tended to be parallel to the electric field.

Example fracture surfaces of hardened PEO/HDDMA with the fracture plane perpendicular to the electric field axis are shown in Fig. 5. The spherulites tended to be more uniformly distributed (less random) than those crystallized without an electric field (compare Fig. 5(a) with Fig. 4(a)). Also, the lamellar planes tended to be more perpendicular to the fracture plane (cf. Fig. 5(b) with Fig. 4(b)).

Optical micrographs using transmitted light of the thin sections of hardened (polymerized) PEO/UDMA (10/90) are shown in Fig. 6. These sections were much more transparent than were those of PEO/HDDMA, possibly because of a similarity between the refractive indices of crystalline PEO and polymerized UDMA. With transmitted light, the PEO phase appeared darker than the hardened UDMA matrix. The PEO crystallinity appears to be a network of crystal lamellae. When crystallized without an electric field, the PEO crystalline network was randomly distributed, as

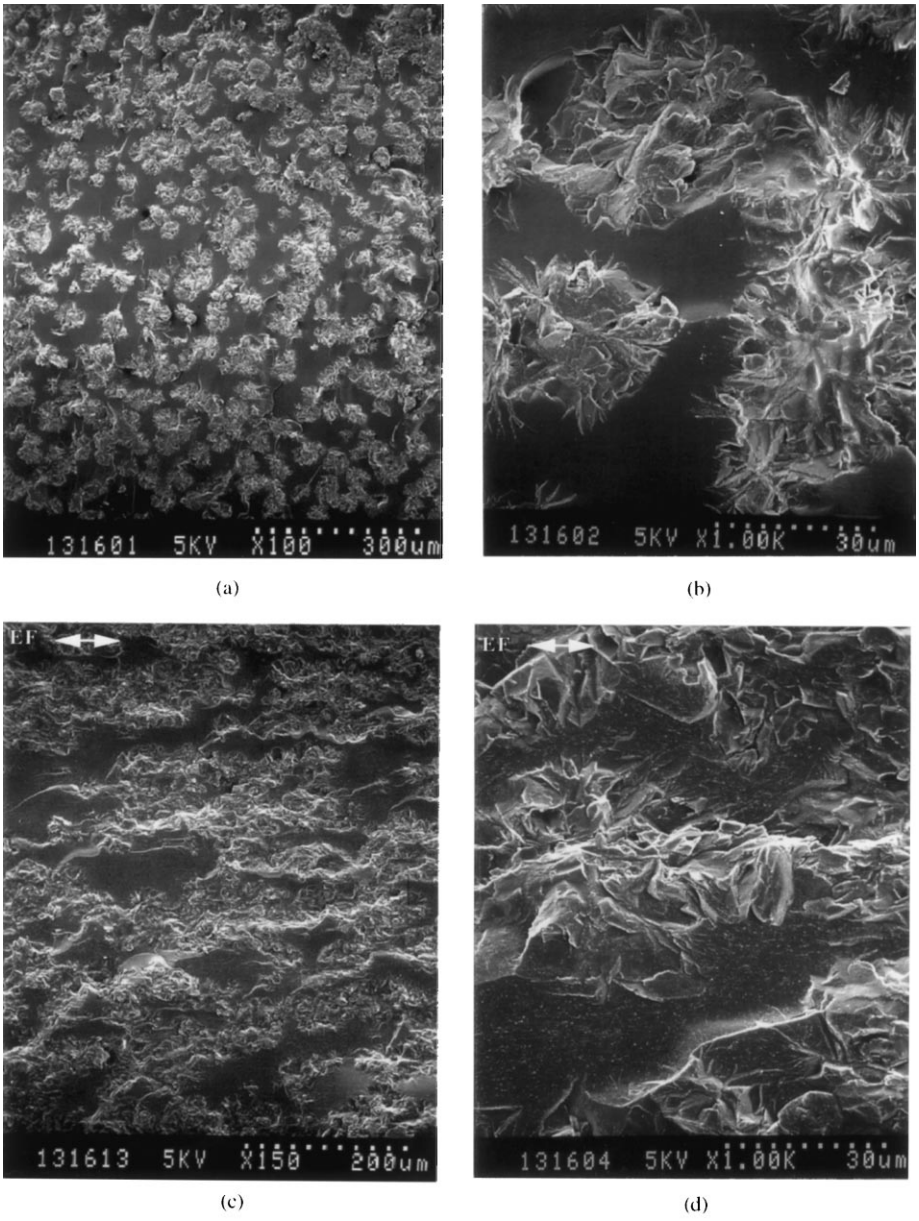

Fig. 4. Scanning electron micrographs of PEO/HDDMA (10/90) mixtures fractured parallel to the electric field. Gelled without ((a), (b)) and with ((c)–(f)) an electric field; polymerized after 3 min under 0.8 kV/mm AC.

seen in Fig. 6(a). But when crystallized (and the matrix hardened) under an electric field, the PEO crystalline network was elongated parallel to the electric field, as shown in Fig. 6(b).

Scanning electron micrographs of fractured surfaces of hardened PEO/UDMA (10/90) are shown in Fig. 7. (The PEO phase appears lighter in color than the hardened UDMA matrix.) PEO crystallized without an electric field is shown in Fig. 7(a) and (b). The PEO phase appears to be mainly fibrillar and occasionally globular. The fibrils are presumably sections through lamellae. The globular material may arise from the surfaces of the lamellae produced by fracture, though the large amount of material in the globules suggests its origin to be thick lamellar stacks. The total amount of PEO visible seems to represent more than its 10% content of the mixture, possibly because the crack path was directed by concentrations of PEO. At higher magnification, Fig. 7(b), the fibrils appear to be part of a branched multi-lamellae structure, often radiating from a common center, as with the starfish-like structure seen at the lower right in Fig. 7(b). The magnified view in Fig. 7(b) also shows small-scale graininess in both the fibrils and globules.

Fig. 7(c) and (d) show fracture surfaces when PEO was crystallized and UDMA hardened under an electric field. The PEO phase again appeared to be mainly fibrillar and

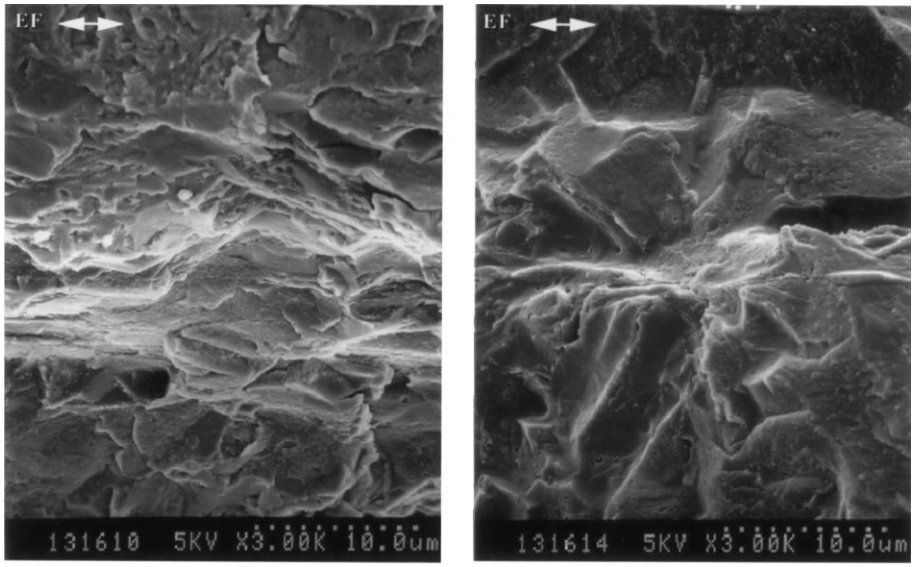

(c) (f)

Fig. 4. (*continued*)

occasionally globular. The total amount of PEO visible, fibrils and globules, now appears to be consistent with its 10% content in the mixture, in contrast to that found without the electric field. Although branching of the fibrils remains, more noticeable is the alignment of the fibrous material with the electric field. All of the fibrils tended to have the same thickness, 1–2 μm, but the fibrils tended to be longer in the field direction (15–20 μm vs. 10 μm or less for the branches) and many appeared not to be branched. However, when branching did occur, it tended to be perpendicular to the field.

3.2. Liquid–liquid phase separation

When an electric field was applied to clear solutions of PEO/HDDMA in the polystyrene cuvets at 68°C, the solutions developed wisps of cloudiness that were roughly aligned with the electric field. The temperature used was well above the solution temperature of PEO in HDDMA, and even above the melting temperature of undiluted PEO (63°C). The onset of the cloudiness depended on the field strength. Under an electric field of 0.13 kV/mm, the cloudiness began after ca. 3 min; under 0.40 kV/mm,

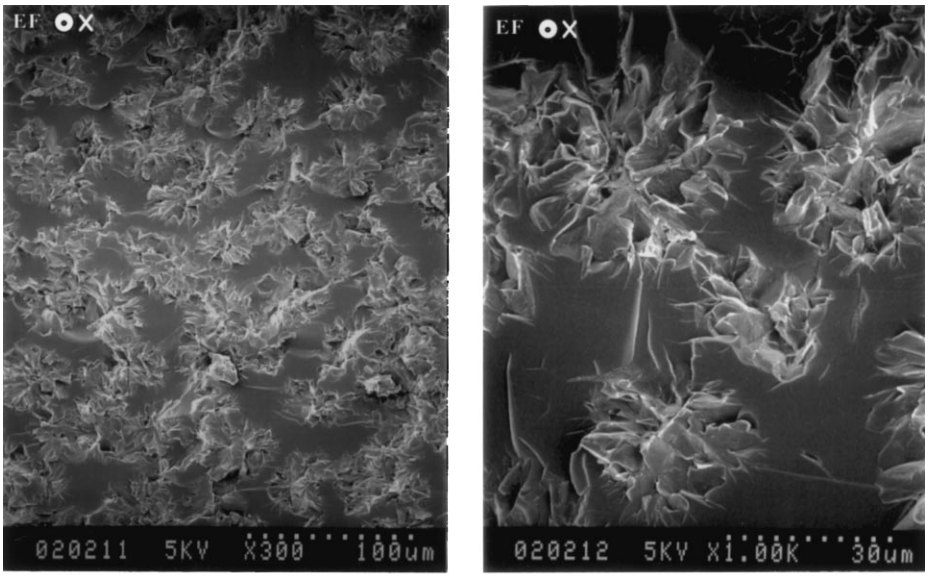

(a) (b)

Fig. 5. Scanning electron micrographs at two magnifications of PEO/HDDMA (10/90) fractured perpendicular to the electric field. Gelled and polymerized after 3 min under 0.8 kV/mm AC.

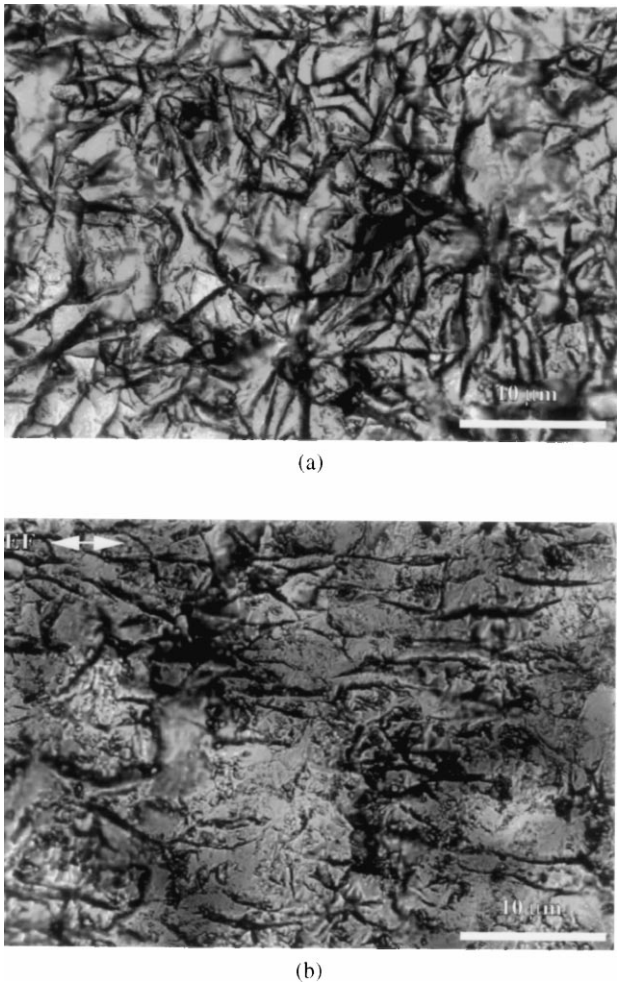

Fig. 6. Optical micrographs of thin sections of PEO/UDMA (10/90) mixtures. Gelled (a) without and (b) with an electric field; polymerized after 30 min (4 min under 0.67 kV/mm AC and 26 min under 0.27 kV/mm AC).

the cloudiness began after 3 s; and under 0.67 kV/mm, the cloudiness began after 1 s. Under an electric field of 0.67 kV/mm, the solution became completely opaque after approximately 3 min. On removing the field, the cloudiness and opacity disappeared, and near-transparency of the solution was restored. The cloudiness was not able to be induced in HDDMA without PEO. When the rate of phase separation (the inverse of the appearance time) was plotted against electric field strength, the curve was parabolic; when the rate was plotted against the square of the electric field strength, a straight line was obtained, as seen in Fig. 8. The cloudiness observed with PEO/HDDMA (10/90) was not observed with PEO/UDMA (10/90).

The PEO phase behavior in the liquid matrices under an electric field was also observed with a light microscope and recorded. Fig. 9 shows examples of this. The PEO was dissolved in HDDMA at 75°C, and a drop of the solution was placed on a glass slide between brass electrodes (spacing: 580 μm). The solution was reheated using a heat gun until the temperature at the electrodes reached 73°C. The PEO started to dissolve after ca. 10 s and was nearly completely dissolved after ca. 30 s. The electric field was applied after 35–40 s, with the temperature remaining at ca. 73°C, and the clock was started. Fig. 9(a) shows the subsequent behavior under an electric field of 2 kV/mm. Several regions of undissolved molten PEO can be seen between the electrodes as darkish, indistinct spots in Fig. 9(a-i), when the field was first applied. These regions had almost disappeared 5 s later (Fig. 9(a-ii)), and then after another 1 s (at 6 s), one of these, about one-third of the width from the right side, reappeared as an arc aligned in the field direction (Fig. 9(a-iii)). The outline of the arc is again relatively indistinct. Other, even less distinct, elongated entities are also visible in the field between the electrodes. These entities may be an agglomeration of globules of a PEO-rich phase.

Fig. 9(b) shows the PEO phase behavior while cooling under an electric field. After placing a drop of the PEO/HDDMA solution on the glass slide between the pair of electrodes and reheating to 73°C, the specimen was allowed to cool toward room temperature. After about 1 min, when the temperature had fallen to ca. 45°C, an electric field of 2 kV/mm was applied, and the clock started. A darkening of the image is seen in Fig. 9(b-i) near the electrodes and moving up the right edge. This may arise from the separation of a PEO-rich phase. Crystallization is seen in Fig. 9(b-ii and iii) to mainly develop in these regions. The crystallinity again appears to have the form of (immature) spherulites. The spherulites formed along the right side appear to be aligned into a string. The spherulites are mainly round in shape, though when the electric field was applied before the temperature began to fall from ca. 70°C, elongated spherulites were formed. Similar, though more muted, behavior was observed with 1 kV/mm.

3.3. Thermal behavior

PEO melting temperatures and crystallinities measured by DSC are summarized in Table 1. Before making the DSC measurement, the mixtures had been cooled in ambient air from 70°C. The melting temperature of the PEO (MW = 20,000) before mixing was 63°C. The PEO melting temperature in PEO/HDDMA (10/90) hardened with and without an electric field was ca. 63°C. The PEO melting temperatures in PEO/UDMA (10/90) hardened without an electric field was also ca. 63°C; that in the PEO/UDMA (10/90) hardened with an electric field was ca. 61°C. The crystallinities of the PEO mixtures were estimated from the heat of fusion, assuming the heat of fusion for the crystalline phase to be 222.6 J/g [22]. The PEO crystallinity before mixing and in PEO/HDDMA (10/90) hardened without an electric field was about 0.70. That in PEO/HDDMA (10/90) hardened with an electric field was 0.61. In contrast, the PEO melting peaks in PEO/UDMA (10/90), whether hardened with or without an electric field, were much smaller than those in PEO/HDDMA (10/90) and not well defined.

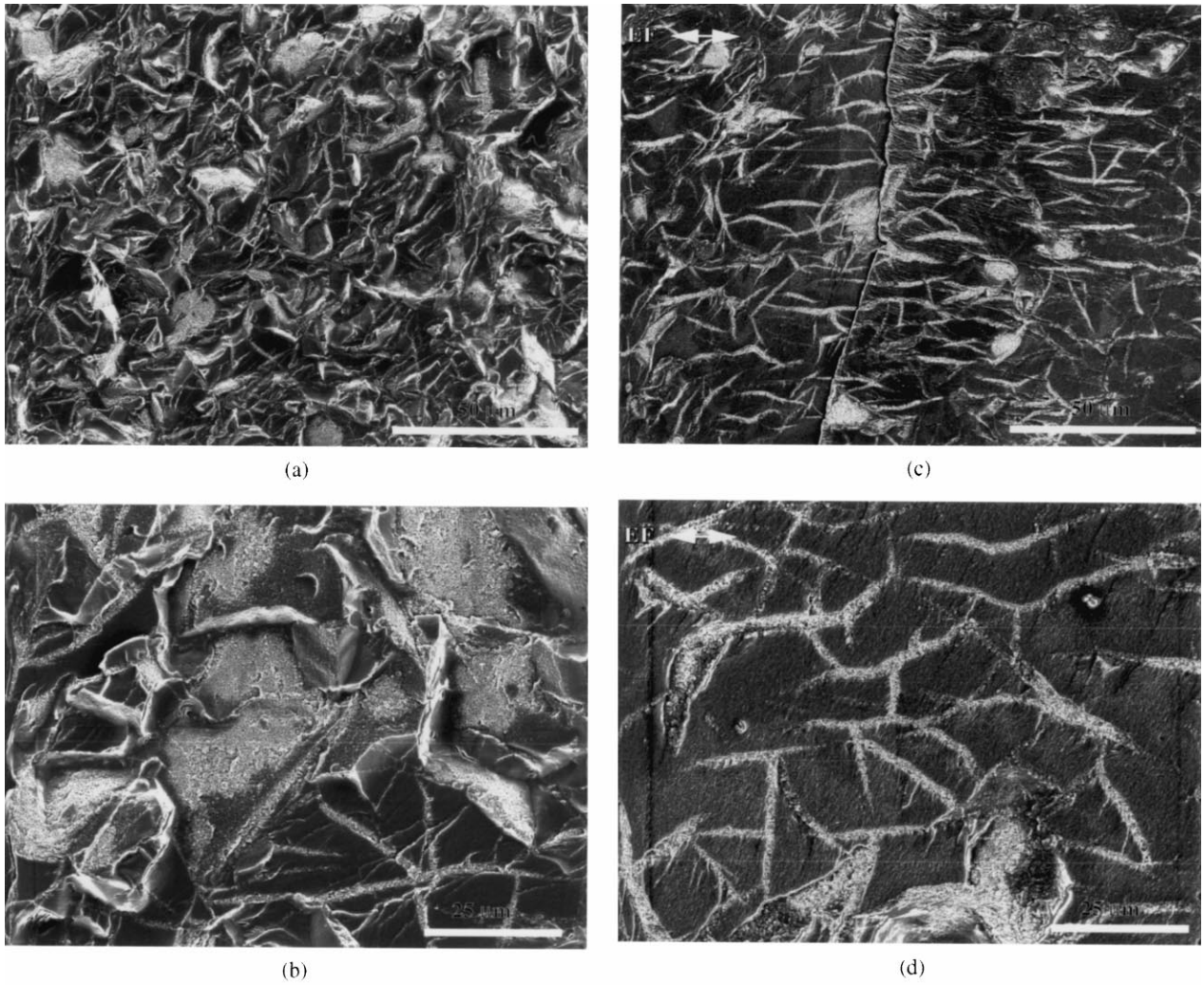

Fig. 7. Scanning electron micrographs of fracture surfaces of PEO/UDMA (10/90) mixtures. Gelled without ((a), (b)) and with ((c), (d)) an electric field, polymerized after 30 min (4 min under 0.67 kV/mm AC and 26 min under 0.27 kV/mm AC).

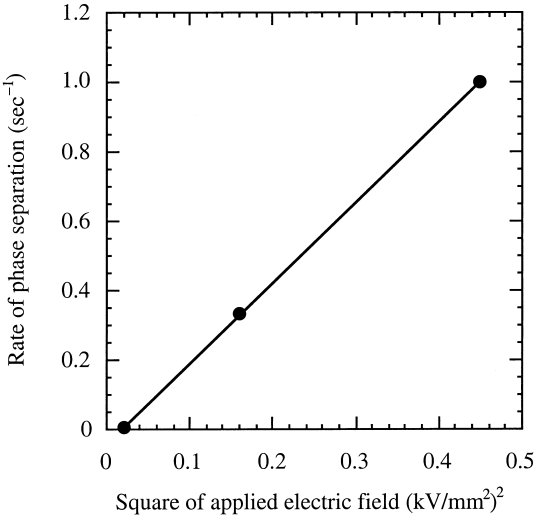

Fig. 8. Rate of phase separation vs. square of the applied electric field. The rate of phase separation is the reciprocal of the delay time between the application of the field and the appearance of phase separation.

3.4. PEO extraction from solidified gels

To examine the extractability of the PEO phase from the hardened gels, specimens was placed in distilled water at room temperature. The weight loss of each was monitored with time, and the loss was found to stabilize for each specimen within 72 h. Each of the specimens had the same shape and size and weighed ca. 35 mg, with the exception of PEO/UDMA crystallized and polymerized under an electric field, which was about half the thickness of the others and weighed ca. 18 mg. The fractional weight losses after 72 h are shown in Fig. 10. The weight losses of PEO/HDDMA (10/90) were more than twice those of PEO/UDMA (10/90). Those hardened under an electric field showed less weight loss than those without an electric field. Having a higher surface to volume ratio, PEO/UDMA crystallized and polymerized under an electric field might have been expected to have the highest fractional weight loss, but it had the least.

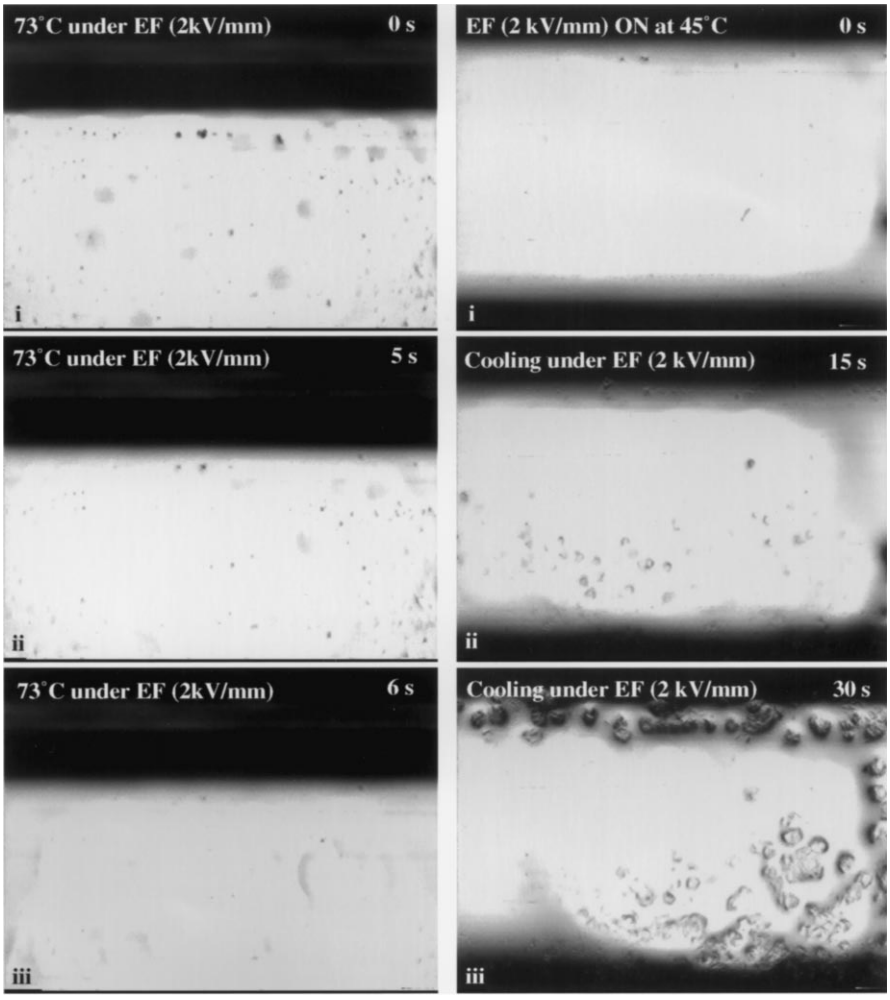

Fig. 9. Snap shots of PEO/HDDMA (10/90) solution under an electric field through an optical microscope. (a) 2 kV/mm AC was applied at 73°C ($>T_m$) for: (i), 0 s; (ii), 5 s; (iii), 6 s. (b) 2 kV/mm AC was applied at 1 min after cooling from 70°C for: (i), 0 s; (ii), 15 s; (iii), 30 s.

3.5. Wide angle X-ray diffraction

To examine the effect of an electric field on the crystalline structure of PEO, X-ray diffraction from the specimen was measured. The soft PEO gel and the hardened PEO mixtures with and without an electric field were scanned at room temperature for both PEO/HDDMA (10/90) and PEO/UDMA (10/90). The results are shown in Fig. 11. The crystalline peaks at 20.2 and 24.1° correspond to PEO. There was no noticeable difference in the location of the these peaks between the two mixtures or between the soft and the hardened gels. The intensity of the peaks from PEO/HDDMA appeared higher than those from PEO/UDMA, and the intensity of the peaks for both gels decreased when the mixtures were hardened under an electric field. The latter, however, may have been caused by the orientation of the PEO crystals. The diffraction scan sampled more of the meridional and less of the equatorial reflections of a PEO fiber pattern.

Table 1
Melting temperatures of PEO; mixtures hardened without and with an electric field (EF)

	T_m(°C)(X_c[a])	
	Without EF	With EF
PEO	63 (0.70)	–
PEO/HDDMA (10/90)	63 (0.70)	63 (0.61)
PEO/UDMA (10/90)	63 (ca. 0.2)	61 (ca. 0.2)

[a] Crystallinity measured from DSC thermogram.

4. Discussion

The phenomena seen with PEO dissolved in and crystallized from two photopolymerizable monomers under electric fields include the alignment of the PEO on crystallization, phase separation at temperatures where the

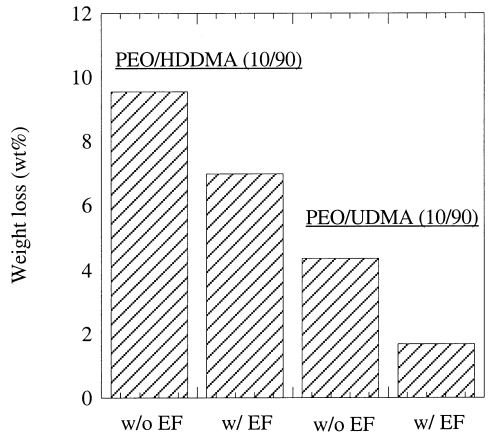

Fig. 10. Extraction of the PEO phase from pieces of hardened specimens after 72 h in water.

components are miscible in the absence of an electric field, retardation of gelation of PEO during cooling, and changes in crystallinity and extractability of the PEO.

4.1. Alignment of spherulites

The alignment of PEO spherulites into groups with a long axis parallel to the field in HDDMA is analogous to the string formation of glass spheres in the same monomer matrix [17,23]. A driving force for alignment of inclusions in a medium under an electric field is a mismatch between the two phases in dielectric constant (for AC) or conductivity (for DC) [24]. Acting against this at low particle concentration is misalignment from Brownian motion or thermal agitation [25]. To achieve alignment, the aligning force must be larger. The ratio of the polarization energy with dissimilar dielectric constants to the thermal agitation energy is given by [26]:

$$\lambda = \frac{\pi \varepsilon_0 \varepsilon_1 a^3 (\beta E)^2}{k_B T} \quad (1)$$

where ε_0 is the permittivity of free space; a the radius of the particles; ε_1 the relative dielectric constant of the liquid resin (about 2.5); β the particle dipole coefficient; E the applied electric field strength; k_B Boltzmann's constant; and T is the absolute temperature. Alignment occurs when λ is greater than one.

For AC fields of sufficiently high frequency, the particle dipole coefficient β is given by $(\varepsilon_2 - \varepsilon_1)/(\varepsilon_2 + 2\varepsilon_1)$, where ε_2 is the relative dielectric constant of the particles. For DC and low-frequency AC fields, the mismatch in conductivity between the particles and matrix may dominate the polarization rather than a mismatch in dielectric constant. Eq. (1) remains the same but β becomes $(\kappa_2 - \kappa_1)/(\kappa_2 + 2\kappa_1)$, where κ_1 and κ_2 are the conductivities of the fluid and particles, respectively [24].

As an example evaluation of Eq. (1), assume that a dielectric constant mismatch dominates polarization. With 4.5 for the dielectric constant of PEO [27,28], 2.5 for the dielectric constant for the liquid resin, 30 μm for the diameter of the PEO spherulites, an electric field of 0.8 kV/mm AC, and a temperature of 45°C (318 K), the ratio of the aligning polarization energy to the misaligning thermal energy, λ is 5.1×10^6. A mismatch in electrical conductivity may dominate the polarization instead. The measured conductivity of HDDMA of 0.30 μS m^{-1} [23] is moderately low. That of PEO, though not measured, is expected to be higher, possibly much higher, as found during dielectric measurements by Connor, Read, and Williams of low molar mass PEO ($M_w < 10^5$) [29]. Although the actual value of λ is reduced by the PEO spherulites in HDDMA not being solid, the polarization, whether from a dielectric or conductivity mismatch, is still expected to dominate thermal agitation,

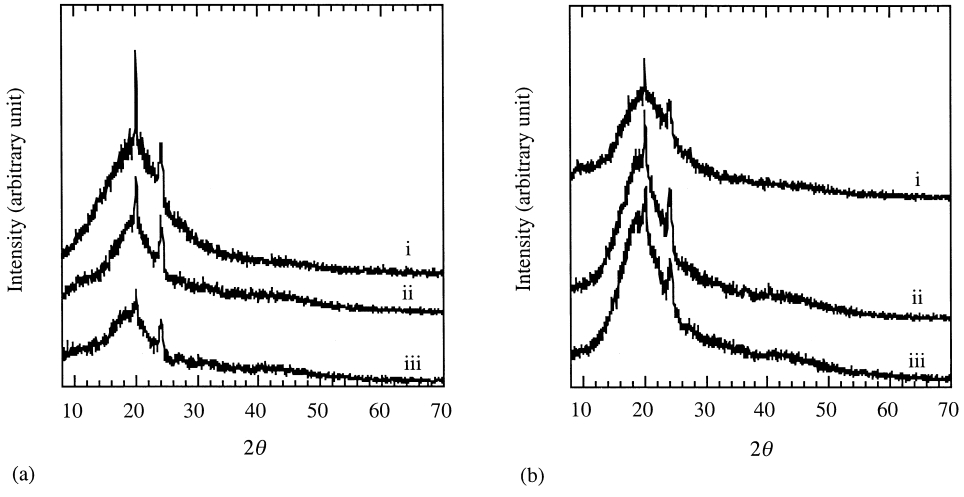

Fig. 11. Wide angle X-ray diffraction: Bragg angle (2θ). (a) PEO/HDDMA (10/90): (i) gel; (ii) hardened without electric field; (iii) hardened with electric field. (b) PEO/UDMA (10/90): (i) gel; (ii) hardened without electric field; (iii) hardened with electric field.

enabling the spherulites to align with each other along the field axis (Fig. 3(b)).

4.2. Alignment of crystalline lamellae

The lamellar crystals within the spherulites were also observed to become aligned with the electric field (Figs. 4 and 5). Even lamellae whose growth was perpendicular to the field direction tended to orient with their planes parallel to the field, as seen in Fig. 4(e) and (f). This alignment arises because the induced polarization of the lamellae by the electric field is highest along the longest plane axis, even when the material is dielectrically isotropic. (With PEO crystallizing as a 7/2 helix [30], its dielectric constant is not expected to be strongly anisotropic.) This is analogous to mica platelets, for example, which were observed to align rapidly under an electric field, with the platelet turning to allow the field to be in the plane of the platelet [17]. Electric field-induced reorientation of lamellar domains in a PS–PMMA diblock copolymer (53 vol% PS) was observed by Amundson et al. [18–20]. Observations were made optically, with small angle X-ray scattering (SAXS) [18,20], birefringence measurement [19], and transmission electron microscopy [20]. Reorientation was shown to minimize the energy [18–20]. Alignment of lamellar planes under an electric field has also been treated analytically by Gurovich [31].

The morphology of the PEO crystallinity that developed in UDMA is somewhat different from that in HDDMA. While the PEO crystallinity developing in HDDMA (Fig. 2(a)) verges on being spherulitic (immature spherulites), that in UDMA was much less spherulitic, with crystalline lamellae having grown in only a few directions (Fig. 2(b)). In the absence of an electric field, the number of directions was several (five, for the group at the lower right of Fig. 7(b)), but with an electric field, the number of directions was often reduced to two, or nearly two. In Fig. 7(c) and (d), the longest lamellae (fibrils in cross-section) in each cluster are aligned with the field. Attached to these are shorter lamellae that seem to be at large angles to the field, suggesting even perpendicularity. This suggests a crystallographic or dendritic relationship between the lamellae, in contrast to the non-crystallographic relationship of lamellae in a spherulite.

4.3. Elongation of crystalline lamellae

In addition to the alignment of the spherulites and crystal lamellae, elongation of the individual spherulites was also observed (Fig. 4(c) and (d)). Field-induced polarization may have a negligible effect on crystal nucleation and growth in the initial stage of crystallization, but it becomes increasingly important as the crystals grow. Polarization increases with the cube of the lamellar size, as seen in Eq. (1), and it may be further enhanced by the platelet shape of the lamellae. The result is that the polarization forces may become large enough compared with the interfacial energy of the lamellar surfaces to lower the secondary nucleation barrier for crystal growth. This would accelerate crystal growth in the field direction in contrast to that in all other directions and would generate elongated spherulites. The seeming effect of the field in allowing dendritic growth but not that in other directions as seen in Fig. 7(d) is less clear. However, the polarization force seems not to affect crystal growth when the applied electric field is below a threshold (such as <0.2 kV/mm for PEO/HDDMA). The threshold field strength for elongating spherulites may provide an indirect index for assessing the secondary nucleation barrier for crystal growth.

4.4. Phase separation

Above the melting temperature of PEO and under an applied electric field, wisps of cloudiness were observed in the PEO/HDDMA solution. With removal of the electric field, the cloudiness disappeared. Some of this behavior was able to be captured with a 2D system, an optical microscope, and video camera. Example frames are shown in Fig. 9.

The onset of the cloudiness occurred sooner with increasing field strength. The rate of appearance in the cuvet cell (the inverse of the appearance time) was linearly proportional to the square of the applied electric field, as seen in Fig. 8. Also proportional to the square of the electric field is the polarization force, as seen in Eq. (1) [25,32]. This suggests that the cloudiness results from a separation of a PEO-rich phase from solution caused by either dielectrophoresis or electrophoresis. Because of either or both a higher dielectric constant or a possibly much higher intrinsic electrical conductivity than the solvent, PEO molecules may congregate into a PEO-rich phase that aligns along the field to lower the Gibbs energy. In addition, solvated PEO molecules in solution may elongate somewhat under the field, thereby reducing their entropy, reminiscent of that occurring in an oriented melt or stretched rubber. This would raise the Gibbs energy of the single-phase solution. Both effects, a lowering of the Gibbs energy of the two-phase mixture through alignment and an elevation of the Gibbs energy of the single-phase mixture through molecular elongation, favor a two-phase mixture.

Field-induced phase separation above the PEO melting temperature was not observed in PEO/UDMA within the observation time, probably because of the higher viscosity of UDMA and perhaps because of better miscibility (solubility) between PEO and UDMA.

4.5. Retardation of gelation

Gelation resulting from PEO crystallization was retarded under an electric field in both the UDMA and HDDMA systems. Also, the gelation of PEO/UDMA was much slower than PEO/HDDMA, most likely because of the higher viscosity of UDMA than that of HDDMA. Higher viscosity may also explain the retardation of gelation under an electric field in HDDMA. By concentrating the PEO in a separate phase, the electric field effectively raises the

viscosity. Although phase separation was not seen with UDMA solutions above the melting temperature of PEO, it may be occurring with both HDDMA and UDMA solutions under crystallization conditions.

Another possible event retarding gelation is local heating. Local heating caused by the slight conductivity of the system could retard crystallization by decreasing the undercooling that is usually needed.

4.6. Crystallinity and extractability of PEO

Heat of fusion measurements (Table 1) showed that the degree of crystallinity was suppressed in PEO/HDDMA when the PEO was crystallized in the presence of an electric field. For PEO/UDMA, the heat of fusion showed that the degree of crystallinity was suppressed both with and without an electric field, the difference between them, if any, being difficult to discern. But the extractability of PEO from the hardened mixtures (Fig. 10) suggests that the electric field suppressed crystallization in both PEO/HDDMA and PEO/UDMA because the extraction was less in both. A reason for associating crystallinity with extractability is that the gelation of the mixtures arising from crystallization implies the development of a crystalline network, and this would provide ready accessibility of the PEO in the interior of the specimen to the surrounding solvent (water). In contrast, amorphous PEO that is molecularly dispersed in the matrix would be relatively inaccessible to dissolution. The concomitant lower extraction and lower crystallinity when UDMA was the matrix instead of HDDMA is consistent with this. The graininess noted on the fracture surfaces of PEO/UDMA (Fig. 7) suggests that the PEO need not be molecularly dispersed to be relatively inaccessible to the external solvent. The graininess indicates envelopment of the phases in one another in this mixture. PEO enveloped by the matrix, probably arising by precipitation as the matrix resin polymerized, would be inaccessible to the external solvent by being surrounded by matrix resin. On the other hand, matrix resin enveloped by the crystalline PEO phase could be carried along with dissolved PEO and overweight the apparent extraction of PEO.

The difference in the crystallinity of the PEO in HDDMA and UDMA with and without the electric field probably arises from same effect of viscosity as that on the retardation of gelation. The phase separation induced by an electric field seen with PEO/HDDMA, and possibly existing also with PEO/UDMA, gives a phase with a concentration of PEO. This phase can be expected to be more viscous than the uniform mixture from which it was derived. Thus, crystallization is inhibited in this electric field-induced phase, and more of the PEO remains uncrystallized when the matrix is polymerized. X-ray diffraction (Fig. 11) showed the same strong crystalline peaks appearing at 20.2 and 24.1° for both PEO/HDDMA and PEO/UDMA. Thus, with and without an electric field, the same PEO crystalline phase seems to be present in all specimens.

5. Conclusions

The application of a high electric field to solutions of 10% PEO in non-polar solvents was found to decrease miscibility, causing in HDDMA a liquid–liquid phase separation at temperatures above the PEO melting temperature and well above the dissolution temperature of PEO in HDDMA. Cooling the HDDMA solution below 45°C induced aligned PEO crystallinity, appearing as aligned groups of the irregular spherulites. When the electric field was above 0.2 kV/mm, the spherulites were elongated, and the lamellae within the spherulites tended to align with their planes in the field direction. From UDMA (a high-viscosity solvent), only branched PEO lamellae formed, with the primary lamellae in the field direction and the few branches at large angles to these, tending to be perpendicular to the field. For both solvents, crystallization was slightly retarded by the field, as was the total amount of crystallinity in HDDMA, and possibly also in UDMA. The PEO crystallinity in UDMA was much less than that in HDDMA, with or without the field, presumably because of viscosity.

Acknowledgements

We thank Prof. Frank E. Filisko and Dr Jaeho Kim for their help in initiating these experiments. This research was supported by Grant P50-DE09296 from the National Institute of Dental Research, National Institutes of Health, Bethesda, Maryland 20892 USA.

References

[1] Tynenska B, Galeski A, Kryszewski M. Polym Bull 1981;4:171.
[2] Moriya S, Adachi K, Kotaka T. Polym Commun 1985;26:235.
[3] Lu FJ, Hsu SL. Macromolecules 1986;19:326.
[4] Marand HL, Stein RS. J Polym Sci, Part B: Polym Phys 1988;26:1361.
[5] Marand HL, Stein RS. J Polym Sci, Part B: Polym Phys 1989;27:1089.
[6] Sterzynski T, Garbarczyk J. J Mater Sci 1991;26:6357.
[7] Shojaie SS, Greenberg AR, Krantz WB. J Membr Sci 1993;79:115.
[8] Hong BK, Jo WH, Hwang IS. Polymer 1999;37:4183.
[9] Taleb M, Didierjean C, Jelsch C, Mangeot JP, Capelle B, Aubry A. J Cryst Growth 1999;200:575.
[10] Venugopal G, Krause S, Wnek GE. J Polym Sci, Part B: Polym Phys 1989;27:497.
[11] Serpico JM, Wnek GE, Krause S, Smith TW, Luca DJ, Laeken AV. Macromolecules 1991;24:6879.
[12] Serpico JM, Wnek GE, Krause S, Smith TW, Luca DJ, Laeken AV. Macromolecules 1992;25:6373.
[13] Ye Y, Wnek GE, Krause S, Smith TW. J Polym Sci, Part B: Polym Phys 1996;34:309.
[14] Morkved TL, Lu M, Urbas AM, Ehrichs EE, Jaeger HM, Mansky P, Russell TP. Science 1996;273:931.
[15] Mansky P, DeRouchey J, Russell TP, Mays J, Pitsikalis M, Morkved T, Jaeger HM. Macromolecules 1998;31:4399.
[16] Köner H, Shiota A, Bunning TJ, Ober CK. Science 1996;272:252.
[17] Park C, Robertson RE. J Mater Sci 1998;33:3541.

[18] Amundson K, Helfand D, Davis D, Quan X, Patel SS, Smith SD. Macromolecules 1991;24:6546.
[19] Amundson K, Helfand E, Quan X, Smith SD. Macromolecules 1993;26:2698.
[20] Amundson K, Helfand E, Quan X, Hudson SD, Smith SD. Macromolecules 1994;27:6559.
[21] Park C, Robertson RE. Dent Mater 1998;14:385.
[22] Wunderlich B. Macromolecular physics. New York: Academic Press, 1973 (p. 388).
[23] Park C, Robertson RE. Mater Sci Engng A 1998;257:295.
[24] Davis LC. J Appl Phys 1992;72:1334.
[25] Pohl HA. Dielectrophoresis: the behavior of neutral matter in nonuniform electric fields. Cambridge: Cambridge University Press, 1978.
[26] Gast AP, Zukoski CF. Adv Colloid Interface Sci 1989;30:153.
[27] Blythe AR. Electrical properties of polymers. Cambridge: Cambridge University Press, 1979 (p. 36).
[28] McCrum NG, Read BE, Williams G. Anelastic and dielectric effects in polymeric solids. New York: Wiley, 1967 (p. 551–561).
[29] Connor TM, Read BE, Williams G. J Appl Chem 1964;14:74.
[30] Miller RL. In: Brandrup J, Immergut E, Grulke EA, editors. Polymer handbook, 4th ed. New York: Wiley-Interscience, 1999 (p. VI–52).
[31] Gurovich E. Macromolecules 1994;27:7339.
[32] Ginder JM. Phy Rev E 1993;7:3418.